### Effect of Algal Biomass on the Properties of Calcium Sulfoaluminate Cement B. Cansu Acarturk<sup>1\*</sup>, Matt A. Jungclaus<sup>1</sup>, Martin Torres<sup>1</sup>, Brooklyn Lash<sup>1</sup>, Wil V. Srubar III <sup>1,2,\*</sup> <sup>1</sup> Department of Civil, Environmental, and Architectural Engineering, University of Colorado Boulder, 1111 Engineering Drive, UCB 428, Boulder, Colorado USA 80309 <sup>2</sup> Materials Science and Engineering Program, University of Colorado Boulder, 4001 Discovery Drive, UCB 027, Boulder, Colorado USA 80303 \*corresponding author, email: wsrubar@colorado.edu **Abstract** Calcium sulfoaluminate (CSA) cement is a low-CO<sub>2</sub> alternative to portland cement (OPC). To further enhance its sustainability, the use of CO<sub>2</sub>-storing algal biomass and algal biochar was explored herein as a carbon-negative cement retarding admixture. CSA cement was replaced with 0, 5, 10, or 15% of raw algal biomass or biochar derived from the raw algal biomass. Results showed that increasing raw algae dosage led to longer delays in the hydration, however, the retardation effect was not observed in samples containing algal biochar due to the absence of hydroxyl and carboxyl functional groups in biochar. Delays in cement hydration due to the incorporation of raw algal biomass corresponded with lower compressive strengths, as anticipated. Despite these reductions, the compressive strengths of the CSA cement pastes were similar to the control OPC pastes, due to the inherently high initial compressive strengths of CSA cement compared to OPC. Both raw algae and biochar effectively lowered the net CO<sub>2</sub> emissions of CSA and OPC, with biochar samples exhibiting lower CO<sub>2</sub> emissions relative to raw algae when normalized for strength performance. Overall, the results suggest that algae may be used effectively with CSA cement for a more workable and sustainable binder system. Keywords: algae, biochar, calcium sulfoaluminate cement, hydration, strength

## 1. Introduction

39

- 40 Ordinary portland cement (OPC) is the most common concrete binder due to its affordability and
- 41 availability [1, 2]. However, the construction industry has been exploring more sustainable alternatives to
- 42 OPC due to the notoriously high carbon dioxide (CO<sub>2</sub>) emissions associated with its production [2].
- 43 Calcium sulfoaluminate (CSA) cement is an alternative cement that exhibits good strength and durability
- 44 properties and lower environmental impacts compared to OPC [3, 4]. CSA cement production requires
- 45 lower kiln temperatures compared to OPC. Additionally, CSA cement contains 20% less calcium than
- 46 OPC. Lower clinkering temperatures and lower calcium content result in a significant reduction of up to
- 47 40% in CO<sub>2</sub> emissions [5]. Apart from its environmental advantages, CSA cement exhibits rapid strength
- 48 development. It can achieve a compressive strength > 20 MPa in only a few hours [5].
- 49 During CSA cement hydration, the main reaction products that form include ettringite and amorphous
- 50 aluminum hydroxide [6-12]:

$$C_4 A_3 \bar{S} + 2C\bar{S} + 38H \rightarrow C_6 A \bar{S}_3 H_{32} + 2AH_3$$
 (1)

$$C_4 A_3 \bar{S} + 18H \rightarrow C_4 A \bar{S} H_{12} + 2AH_3$$
 (2)

- The hydration of CSA cement relies on the presence and reactivity of ye'elimite  $(C_4A_3\bar{S})$ , calcium sulfate 51
- $(C\bar{S})$ , and water (H). During CSA cement hydration, ettringite  $(C_6A\bar{S}_3H_{32})$  begins to form within the first 52
- 53 few hours in the presence of  $C\bar{S}$  (see Eq. 1) and leads to significant microstructural development within
- 24 hours [6, 11]. Once  $C\bar{S}$  is depleted, the formation of monosulfate  $(C_4A\bar{S}H_{12})$  takes place instead of 54
- ettringite (see Eq. 2). Due to the fast formation of the ettringite, the hydration process of CSA cement has 55
- 56 a much faster reactivity than OPC, leading high heat release within two hours, rapid setting, and high
- 57 early strength gain [8].
- 58 The use of CO<sub>2</sub>-storing additives, such as biomass or biochar, has been shown to further reduce CO<sub>2</sub>
- 59 emissions related to cement production without compromising its strength or durability characteristics
- 60 [13-18]. Biomass sources include wood waste, coconut shell, nut residue, cotton stalk, and dairy manure
- 61 [14, 19, 20]. In addition to agricultural sources, algal biomass can also contribute to carbon capture and
- utilization by incorporating captured CO<sub>2</sub> into the biomass during photosynthesis. In general, 100 g of 62
- algal biomass captures ~ 180 g of CO<sub>2</sub> [21]. Some studies have shown that use of algal biomass can 63
- 64 improve the strength of the cementitious samples because of early age interactions between algae and
- 65 water. Dry algae could limit water availability for cement hydration by absorbing water during the early
- 66 stages of cement hydration. This absorbed water could be released at later ages to assist ongoing
- hydration, similar to the behavior of internal curing agents such as saturated lightweight aggregates and 67
- superabsorbent polymers [13, 22]. Additionally, concrete samples infused with brown algae extract 68
- 69 demonstrated comparable strength while exhibiting improved durability, particularly in resisting chloride
- 70 diffusion [23]. Biochar is produced from biomass through pyrolysis (i.e., heating the biomass under
- 71 oxygen-limited conditions), resulting in the decomposition of organic matter and the production of a more
- 72 stable carbon-rich material [16, 24]. Fine biochar particles function as a micro-filler in cement and finer
- 73 cement grains exhibit rapid and complete hydration, enhancing cement paste's degree of hydration and
- 74 reaction kinetics when incorporating a micro-filler [24, 25]. These fine biochar particles, being smaller
- 75 than cement grains and macro pores, promote early-stage hydration by acting as a filler effect, and lead to
- 76 accelerated setting and solid network percolation. This effect increases the ability of biochar to block
- 77 macro pores in the mortar, resulting in a compacted hardened mortar, improved strength performance [14,
- 78 24].
- 79 A prior investigation involving Chlorella algae demonstrated that incorporating raw algae into OPC paste
- 80 resulted in a notable retardation of hydration reactions [13]. A mere 1% addition of raw algae by cement
- 81 weight led to an 83% delay yet had no adverse impact on the strength at 28 days. In another study, Lin et

al. [17] incorporated *Chlorella* algae in OPC mixtures at concentrations between 0.5 and 15% and observed an occurrence of significant strength reduction at dosages greater than 5% and a permanent hindering effect on hydration. These retardations and hindering effects were attributed to the functional groups present in algae, which slowed down the hydration of alite phase in OPC, consequently delaying or even preventing the formation of calcium silicate hydrate [13, 17]. However, the retardation effect was eliminated when algae was subjected to heat treatment to obtain biochar, likely due to the breakdown of functional groups at high temperatures [13].

Despite promising findings in the study of algal biomass in OPC systems, no research has neither explored the use of algal biomass in CSA cement nor investigated impact of raw algae on CSA cement hydration and property development. To address this gap, this study assessed the impact of using raw *Chlorella* algae or its biochar as a functional filler in CSA cement pastes. More specifically, this research investigated the effects of *Chlorella* algal biomass on the hydration kinetics, setting time, microstructure development, and compressive strength. The investigation involves varying levels of algal biomass, specifically 0%, 5%, 10%, and 15%, as replacements for CSA cement. First, isothermal calorimetry was utilized to analyze the hydration kinetics and the Vicat needle test was conducted to determine the setting times of the samples. Second, compressive strength of samples was measured at 1, 7, and 28 days. After compressive strength testing, the samples were analyzed using thermogravimetric analysis and scanning electron microscopy for phase development and morphology, respectively. Additionally, life cycle assessment (LCA) was utilized to estimate the cradle-to-gate embodied carbon emissions (kgCO<sub>2</sub>e), biogenic carbon storage (kgCO<sub>2</sub>), and net CO<sub>2</sub> emissions (kgCO<sub>2</sub>e) for each mix design including the functional performance.

## 2. Materials and Methods

## 2.1. Materials

CSA cement sourced from Buzzi Unicem and OPC (Quikrete Type I/II cement) were used for all paste mixtures. The cement oxide compositions, measured using X-ray fluorescence (XRF) at Hazen Analytical, are shown in **Table 1**. Deionized water (18 kOhm) was used for all paste mixtures. For the algal biomass, *Chlorella* algae pellets obtained from Earth Circle Organics were processed by grinding them with a mortar and pestle until they passed through a 125 µm sieve.

**Table 1:** X-ray fluorescence oxide compositions for OPC and CSA cement.

Oxides	CSA (wt. %)	OPC (wt. %)
$Al_2O_3$	21.7	4.58
CaO	43.0	61.5
Fe <sub>2</sub> O <sub>3</sub>	1.80	3.81
K <sub>2</sub> O	0.20	0.622
MgO	1.10	1.00
MnO	0.08	0.23
Na <sub>2</sub> O	0.10	0.15
P <sub>2</sub> O <sub>5</sub>	0.20	0.170
SiO <sub>2</sub>	7.20	19.6
SO <sub>3</sub>	20.7	3.39
TiO <sub>2</sub>	0.60	0.19
LOI	1.50	2.86

## 2.2. Experimental Methods

112113

129

## 2.2.1. Sample Preparation

- 114 Two sets of CSA cement paste samples were used in the experiments. The first set contained algae in its
- raw, dry, and untreated form, while the second set contained algae that had undergone a heat treatment to
- obtain a biochar. To produce the biochar, the ground *Chlorella* algae powder was heated in an oxygen-
- limited muffle furnace from 25 °C to 300 °C and held at 300 °C for 1 hour [13]. The temperature of 300
- °C was selected to ensure complete thermal decomposition of *Chlorella* [13, 26].
- 119 CSA cement pastes were prepared using raw algae and biochar at a water-to-cement ratio (w/c) of 0.40.
- Algal biomass was added to the cement in concentrations of 5%, 10%, and 15% by mass, replacing an
- equivalent amount of CSA cement. CSA cement and OPC pastes without any algae addition were used as
- 122 control mixtures. To ensure appropriate workability of the mixtures, a superplasticizer (polycarboxylate
- ether) was added to all mixtures at a dosage of 0.5% by weight of cement. Similarly, 0.5% citric acid
- (Alfa Aesar, 99%) by cement weight was used as a retardant in CSA mixtures in accordance with
- previous research [27]. Mixture formulations and sample nomenclature are shown in **Table 2**. In the
- 126 context of this study, CSA samples are denoted as follows: 'C' represents CSA cement, 'A' represents
- algae, 'B' represents biochar, and 'c' represents citric acid. The numbers following these notations
- represent the percentage of CSA cement, algae, or biochar used in the mixtures.

**Table 2:** Sample nomenclature and mixture proportions for 100 g paste samples.

Sample	Cement (g)	Algae/ Biochar (g)	SP (g)	Citric Acid (g)	Water (mL)	w/c Ratio
OPC	100	0	0.5	0	40	0.4
C100	100	0	0.5	0	40	0.4
C100-c	100	0	0.5	0.5	40	0.4
A5C95	95	5	0.5	0	40	0.4
A10C90	90	10	0.5	0	40	0.4
A15C85	85	15	0.5	0	40	0.4
A5C95-c	95	5	0.5	0.5	40	0.4
A10C90-c	90	10	0.5	0.5	40	0.4
A15C85-c	85	15	0.5	0.5	40	0.4
B5C95	95	5	0.5	0	40	0.4
B10C90	90	10	0.5	0	40	0.4
B15C85	85	15	0.5	0	40	0.4
В5С95-с	95	5	0.5	0.5	40	0.4
В10С90-с	90	10	0.5	0.5	40	0.4
В15С85-с	85	15	0.5	0.5	40	0.4

### 130

131

## 2.2.2. Raw Algal Biomass and Biochar Characterization

- In order to determine the morphology and chemical composition of raw and heat-treated algae powders, algae particles were analyzed using scanning electron microscope (SEM) and Fourier-transform infrared
- 134 (FTIR) spectroscopy. The morphology of raw algae and algal biochar particles was analyzed using a
- Hitachi SU3500 SEM operating in secondary electron imaging mode at 10 kV. Prior to imaging, samples
- were coated with a platinum film of approximately 10 nm under vacuum (<0.15 mb) to prevent charging.

137 Raw algae and algal biochar particles were analyzed using an attenuated total reflectance (ATR) FTIR

(ThermoScientific Nicolet iS20 FTIR). Each spectrum was an average of 64 measurements, scanned from

139 2000 to 600 cm<sup>-1</sup> at a resolution of 4 cm<sup>-1</sup>.

138

143

144

153 154

140 FTIR was used to determine the chemical composition and functional groups present within the raw algal 141

biomass and to determine changes in these groups with heat treatment upon conversion to biochar. The

results are presented in Figure 1. Various functional groups were observed, including C=O in -COOH 142

(1725 cm<sup>-1</sup>), C=O stretch in ketone and carbonyl acid (1650 cm<sup>-1</sup>), C=C (1535 cm<sup>-1</sup>) and C-OH (1059

cm<sup>-1</sup>) [13, 17, 20, 28]. Carboxyl and hydroxyl functional groups, among the identified structures, have

been found to retard the OPC hydration [13, 29, 30]. 145

Raw algae samples had significant peaks at 1725 cm<sup>-1</sup> and 1060 cm<sup>-1</sup> which are attributed to the carboxyl 146

147 and hydroxyl groups. However, the disappearance of these peaks was observed in the biochar sample.

148 During the heat treatment process to form biochar, the raw algae experiences a series of chemical and

149 physical reactions. As the temperature rises, typically above 300 °C, the biopolymers present in algae,

150 including proteins, lipids, and carbohydrates, begin to decompose, resulting in the release of carbon

dioxide. This reaction is associated with the breaking and reconfiguration of C=O and -COOH functional 151

152 groups within the biopolymers, as shown in **Figure 2**.

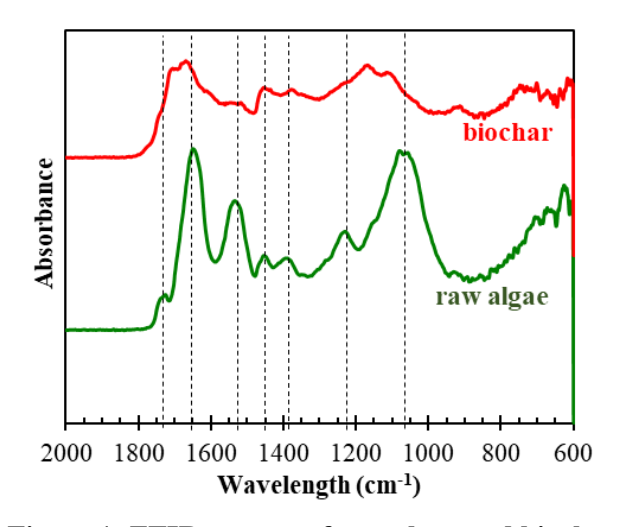


Figure 1: FTIR spectra of raw algae and biochar.

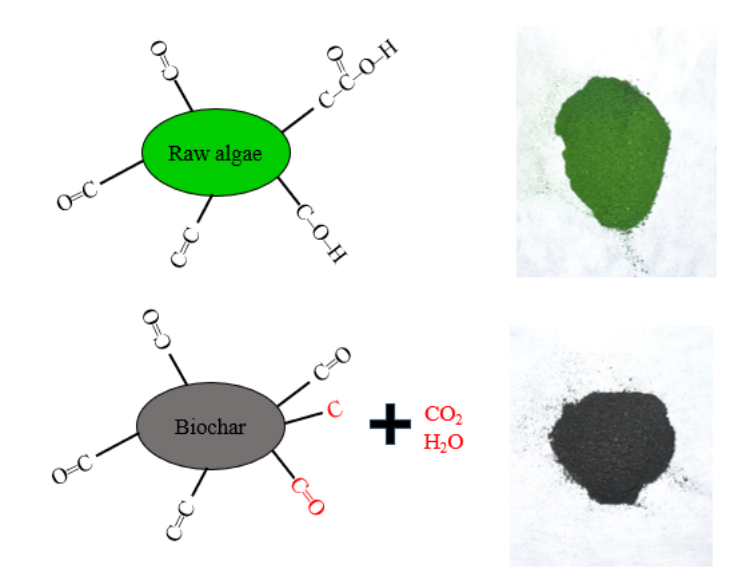


Figure 2: Schematic representations and photographs of raw algae and biochar.

The morphological characteristics of the raw algae and biochar were investigated using SEM and displayed in **Figure 3**. The raw algae exhibited rough surfaces composed of small-sized particles ranging between 5-50 µm (**Figure 3a**). However, biochar sample had smoother surfaces as a result of the heat treatment, possibly linked to the disappearance of the -OH and -COOH functional groups (**Figure 3b**).

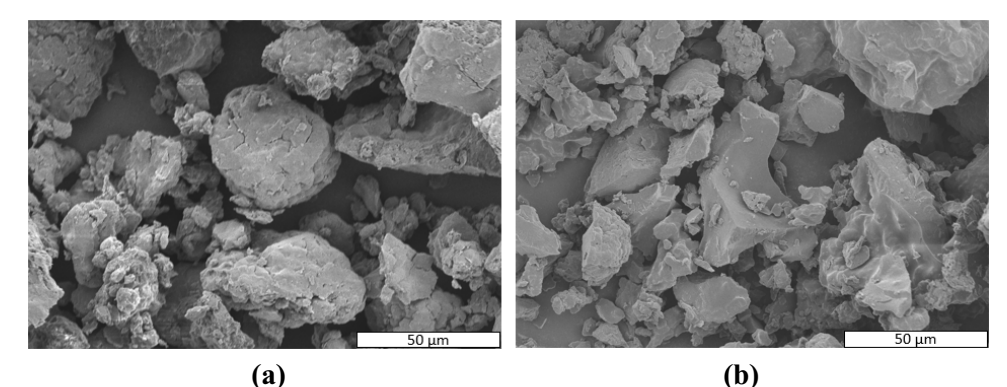


Figure 3: Morphology of the (a) raw algae and (b) biochar.

### 2.2.3. Hydration Kinetics, Setting Time, and pH Measurements

CSA cement pastes without and with raw algae or algal biochar for isothermal calorimetry were prepared using the procedures outlined in ASTM C1679 [31]. Approximately 25 g of paste were mixed using a Hamilton Beach 6-speed hand mixer, first at the lowest speed for 30 seconds and then at the highest speed for 90 seconds. After mixing, 5g of each paste was transferred into a glass ampoule, sealed, and placed into a TAM AIR calorimeter to track heat evolution for 24 hours. All samples were placed into the calorimeter within 2-3 minutes of water-cement contact. The temperature was maintained at 25°C throughout testing. The generated heat was collected using TAM AIR software and the heat evolution and total cumulative heat were normalized by per gram of cement.

To determine setting time, CSA pastes were prepared in accordance with ASTM C305 [32]. The assessment of initial and final setting times was conducted using a Vicat needle apparatus, according to

- ASTM C191 [33]. Each sample underwent duplicate tests to measure initial and final setting times, and
- the results were averaged.

187

- Dilute cement paste samples were prepared using a w/c ratio of 2.0 to track pH change of CSA samples
- without and with raw algae or biochar. Cement, water, and 15% raw algae or 15% biochar were placed in
- a beaker and stirred continuously using a stir plate at 400 rpm until testing. Measurements commenced 5
- minutes after mixing and continued until the onset of sample hardening. The duration of this measurement
- phase varied depending on the sample type: approximately 30 minutes for control and biochar samples,
- and about 45 minutes for samples containing raw algae. The pH of the solution was measured using a pH
- meter (Mettler Toledo, Seven Compact).

## 2.2.4. Compressive Strength

- 188 CSA cement pastes without and with raw algae or algal biochar were prepared for compressive strength
- testing. Additionally, one set of OPC mixture were prepared to compare the strength development of CSA
- mixtures containing raw algae or algal biochar with OPC (see Table 2). For each mixture, a set of 1 cm<sup>3</sup>
- cubes were prepared according to a modified ASTM C305 [32]. The same mixing procedure described in
- Section 2.2.3 was followed to mix samples. After mixing, cement paste samples were placed into 1 cm<sup>3</sup>
- molds, cured at  $\sim 23$  °C and 100% relative humidity (RH) and demolded after 24 hours. The 1-day
- samples were tested immediately following their removal from the molds. The remaining samples were
- kept in 100% RH environment until further testing. Compressive strength was characterized at 1, 3, 7, 28,
- 196 56, and 90 days in accordance with ASTM C109 [34] using an Instron Universal Testing machine with a
- 197 50 kN load cell and a 0.1 mm/sec compression rate. Samples were tested in triplicate.

# 198 2.2.5. Morphology and Microstructural Phase Development

- Morphology and microstructural phase development of control samples and samples containing 15% raw
- algae and 15% algal biochar were examined using SEM as described in Section 2.2.2 and
- thermogravimetric analysis (TGA), respectively. Following compressive strength testing, the samples
- were ground using a mortar and pestle until they could pass through the No. 100 (149 µm) sieve and
- immersed in isopropanol for a duration of 20 ± 2 hours, followed by drying at 40 °C for a period of 3-4
- hours in order to stop hydration [35, 36]. This method for hydration arresting was chosen with the aim of
- 205 reducing the water loss from ettringite and monosulfate phases while controlling the drying time to limit
- the carbonation [36, 37]. Thermal analysis of the samples was conducted using a Discovery TGA 5500.
- Approximately 30 mg of samples were heated at a rate of 10 °C/min from 25 °C to 1000 °C under
- 208 nitrogen in alumina crucibles. The mass loss was used to calculate the proportions of calcium aluminate
- 209 hydrate phases, specifically ettringite (AFt) and monosulfate (AFm), as well as aluminum hydroxide
- 210 (AH<sub>3</sub>) in the samples. The differential mass loss versus time curve was plotted to determine the changes
- in the amount of hydration products with increasing temperature.

## 212 **2.2.6.** Life Cycle Assessment

- 213 The effect of raw algal biomass and algal biochar on the embodied carbon emissions (kgCO<sub>2</sub>e) of each
- mix design was estimated using a screening life cycle assessment (LCA) meeting ISO 14040/14044
- standards [38, 39]. This LCA was conducted to assess the cradle-to-gate emissions and biogenic carbon
- storage for various concrete mix designs, as defined in Table 2. The results of this analysis are intended to
- inform future research and development of concrete mixtures using algal biomass and biochar by
- 218 elucidating the potential embodied carbon emissions and biogenic carbon sequestration associated with
- these mixtures and their respective compressive strengths.
- The declared unit of the assessment was one kilogram of the CSA cement mixture, and functional
- 221 performance is defined by the properties of each mix design shown in **Table 2** as well as the experimental

compressive strength of each mixture defined herein. Results were calculated in terms of embodied carbon emissions per unit mass (kgCO<sub>2</sub>e/kg) and embodied carbon emissions per strength-normalized unit mass (kgCO<sub>2</sub>e/kg-MPa), taking into account the experimental compressive strength determined as part of this study. The system boundary included life cycle modules A1-A3, representing cradle-to-gate embodied carbon emissions, and module D, representing biogenic carbon storage. Cradle-to-gate emissions refer to the emissions that result from material extraction, transportation, and manufacture. Biogenic carbon storage refers to the CO<sub>2</sub> stored in natural materials, including CO<sub>2</sub> storage resulting from photosynthesis [40]. There is no commonly agreed upon accounting scheme for incorporating biogenic carbon storage, so, for the purposes of this study, biogenic carbon storage was included in life cycle module D.

All constituent materials included in the mix designs described in **Table 2** will be evaluated. Embodied carbon coefficients (ECCs) for each constituent material were extracted from prominent life cycle inventory databases [41, 42], environmental product declarations [43], and scientific literature [44, 45]. The cradle-to-gate ECCs (ECC<sub>A1-A3</sub>, kgCO<sub>2</sub>e/kg-material) identified are provided in units of 100-year global warming potential (GWP-100, kgCO<sub>2</sub>e), which is a commonly used measure of environmental impacts which normalizes the impacts of various greenhouse gases based on the 100-year global warming impact of CO<sub>2</sub>. Biogenic carbon storage ECCs (ECC<sub>D</sub>, kgCO<sub>2</sub>/kg-material) are provided as a measure of stored CO<sub>2</sub>. All ECCs used in the LCA are shown in **Table 3**.

**Table 3:** ECCs corresponding to life cycle modules A1-A3 and D (biogenic carbon storage) for the constituent materials of all mixtures.

Material	ECC <sub>A1-A3</sub> (kg-CO <sub>2</sub> e/kg- material)	ECC <sub>D</sub> (kg-CO <sub>2</sub> e/kg- material)	Source
CSA Cement	0.673	0.000	[45]
OPC	0.970	0.000	[41]
Raw algal biomass	0.085	-1.800	[13, 45]
Algal biochar	0.230	-2.930	[42]
DI Water	0.000344	0.000	[41]
Polycarboxylate ether superplasticizer	1.880	0.000	[41]
Citric acid	3.100	0.000	[44]

243 The carbon emissions for each concrete mix are calculated according to:

$$EC_{mix,A1-A3} = \sum_{i=1}^{n} (m_i * ECC_{A1-A3,i})$$
 (3a)

$$EC_{mix,bio} = \sum_{i=1}^{n} (m_i * ECC_{D,i})$$
(3b)

where  $m_i$  is the mass in kilograms of constituent material, i, per kilogram of mix (kg-material/kg-mix),  $ECC_{i,A1-A3}$  is that material's cradle-to-gate embodied carbon ECC (kgCO<sub>2</sub>e/kg-material),  $ECC_{i,D}$  is that

- material's biogenic embodied carbon coefficient (kgCO<sub>2</sub>e/kg-material), n is the total number of
- constituent materials in the mixture,  $EC_{mix,AI-A3}$  is the total cradle-to-gate embodied carbon emissions of
- one kilogram of mix (kgCO<sub>2</sub>e/kg), and  $EC_{mix,D}$  is the total biogenic carbon storage of one kilogram of mix
- 249 (kgCO<sub>2</sub>/kg). The net CO<sub>2</sub> emissions can be calculated simply as:

$$EC_{mix,net} = EC_{mix,A1-A3} + EC_{mix,D} \tag{4}$$

where  $EC_{mix,net}$  refers to the net  $CO_2$  emissions of each mixture.

#### 3. Results and Discussion

251

252

## 3.1. Hydration Kinetics and Setting Time

- 253 Isothermal calorimetry was used to characterize the hydration kinetics of CSA cement pastes with
- increasing dosages of raw algae and biochar, both with and without citric acid addition. The effects of
- each replacement level on timing of the primary hydration reactions and on the cumulative heat release
- were evaluated over the first 24 hours of hydration. Although heat release was tracked over the 24 hours,
- Figures 4a and 5a were truncated to provide more clarity to earlier age reactions as little heat release
- occurred between 4 and 24 hours.
- Figure 4a shows the rate of heat release results of raw algae samples over time. The CSA sample without
- retarder, labeled as C100, was employed as the control sample and is denoted by the black curve in both
- Figures 4a and 5a. In this C100 sample, a rapid and substantial heat release occurred, peaking at 15
- 262 minutes, attributed to the formation of the ettringite phase. This peak was followed by a sudden decrease,
- 263 potentially due to the transformation from non-crystalline hydration products to crystalline ettringite or
- 264 consumption of the ye'elimite phase [7]. The A5C95 sample exhibited a behavior quite akin to that of the
- 265 C100 sample, likely owing to its low proportion of raw algae.
- On the other hand, the rate of heat release curves for the A10C90 and A15C85 samples indicated that
- increasing algae replacement resulted in a reduction in the rate of heat release and slight retardation in the
- 268 timing of the main hydration peaks within the mixtures containing 10% and 15% algae. Although this was
- a slight retardation, it accounted for 50% and 100% increased retardation compared to the control sample,
- 270 C100 (**Table 4**). It is also important to note that the incorporation of algae within the CSA cement
- samples did not lead to prolonged retardation as observed in OPC in previous studies, where the addition
- of just 1% raw algae into OPC led to a 7-hour increase in hydration time compared to the control [13, 17].
- Prior research has demonstrated that algal biomass primarily retards alite hydration and slightly affects
- belite hydration [13, 17]. Thus, the comparatively lesser retardation observed here aligns with the
- 275 understanding that CSA cement lacks the alite phase.
- 276 The addition of citric acid was found to retard the initiation of hydration in both CSA cement (C100-c)
- and CSA cement combined with raw algae samples (A5C95-c, A10C90-c, A15C85-c) with respect to
- 278 C100 sample. Using citric acid resulted in a delayed occurrence for the main heat release peak, coupled
- with a decrease in the maximum rate of heat release. Citric acid primarily delays ettringite formation by
- adsorbing onto the surface of ettringite crystals, effectively blocking their growth and preventing further
- precipitation [46]. Additionally, citric acid could bind calcium or alumina ions, inhibiting the dissolution
- of ye'elimite and its subsequent reaction to form ettringite [47]. Citric acid used in combination with raw
- algae further prolonged the hydration timing, suggesting a synergistic effect. The highest raw algae
- replacement level yielded a hydration time of 55 minutes, as indicated in **Table 4**.
- 285 The cumulative heat evolved by CSA cement containing raw algae, with and without citric acid over, 24
- 286 hours is shown in **Figure 4b**. In general, cumulative heat release was inversely correlated with the raw
- algae replacement level, as well as the level of retardation. C100 and A5C95 samples showed higher total

heat evolution compared to samples with higher replacement level and citric acid. The mixtures involving citric acid exhibited lower cumulative heat release than their counterparts without citric acid, potentially attributed to the lower reactivity observed in mixtures with higher algae dosages.

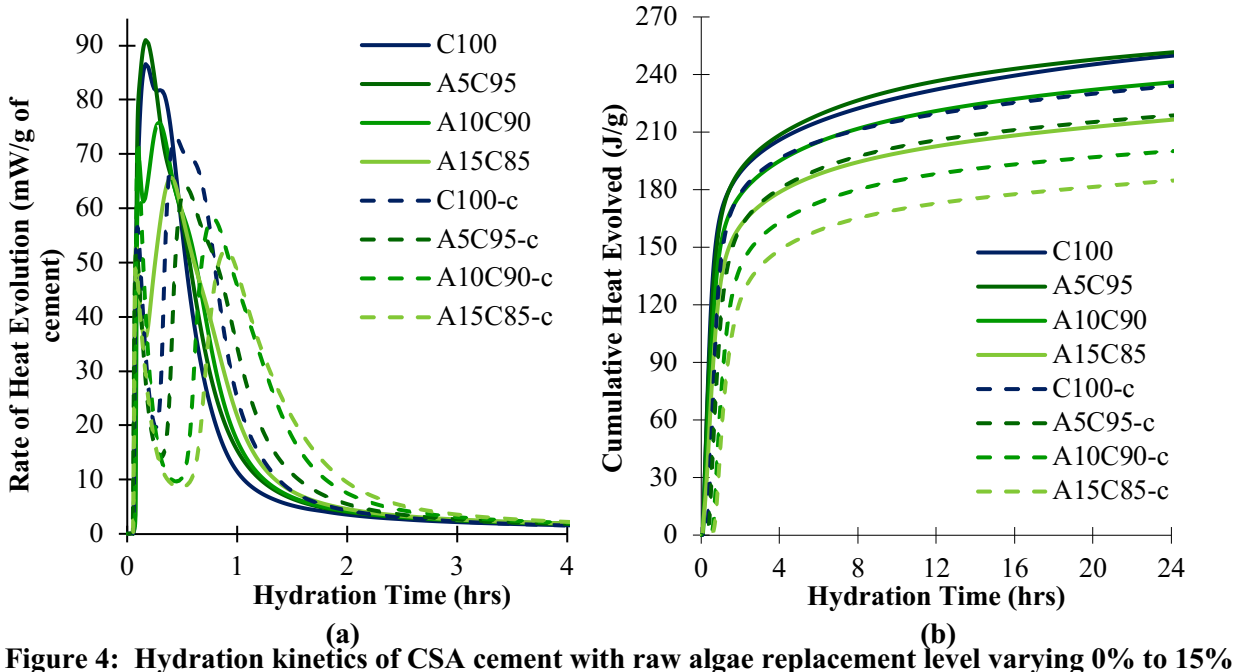


Figure 4: Hydration kinetics of CSA cement with raw algae replacement level varying 0% to 15% and with and without citric acid: (a) Rate of heat evolution; (b) Cumulative heat evolution (A: raw algae, C: CSA cement, c: citric acid).

Hydration kinetics of biochar samples without citric acid are shown in **Figure 5a** which displays that addition of biochar did not change the timing of the main hydration peak but did slightly decrease the rate of heat release. Increasing biochar dosage did not cause increased retardation, as occurred in raw algae samples described above, the highest retardation amount observed was only 42% longer than the control with 10% addition of biochar (**Table 4**). These findings are indicative of the decomposed functional groups within the biochar, which did not induce significant retardation in biochar mixes.

Compared to no citric acid samples, addition of citric acid retarded the hydration reactions independently of the biochar amount. The use of citric acid in biochar samples resulted in very slight retardation when biochar dosage was increased. Hydration time of 37 minutes was obtained with the highest replacement level (**Table 4**). Raw algae and citric acid appeared to work synergistically, whereas biochar and citric acid exhibited independent effects.

The cumulative heat release of biochar and CSA mixtures over 24 hours is shown in **Figure 5b**. When biochar dosage increased in the samples without citric acid, the maximum rate of cumulative heat release decreased. However, no significant decrease was observed between the samples B10C90 and B15C95, the total heat for all these samples remained approximately the same around 230 J/g as summarized in **Table 4**. Addition of citric acid resulted in a slight decrease in the cumulative heat release with increasing biochar replacement level. When compared to raw algae mixtures with citric acid, biochar mixtures with citric acid led to greater cumulative heat release as shown in Table 4.

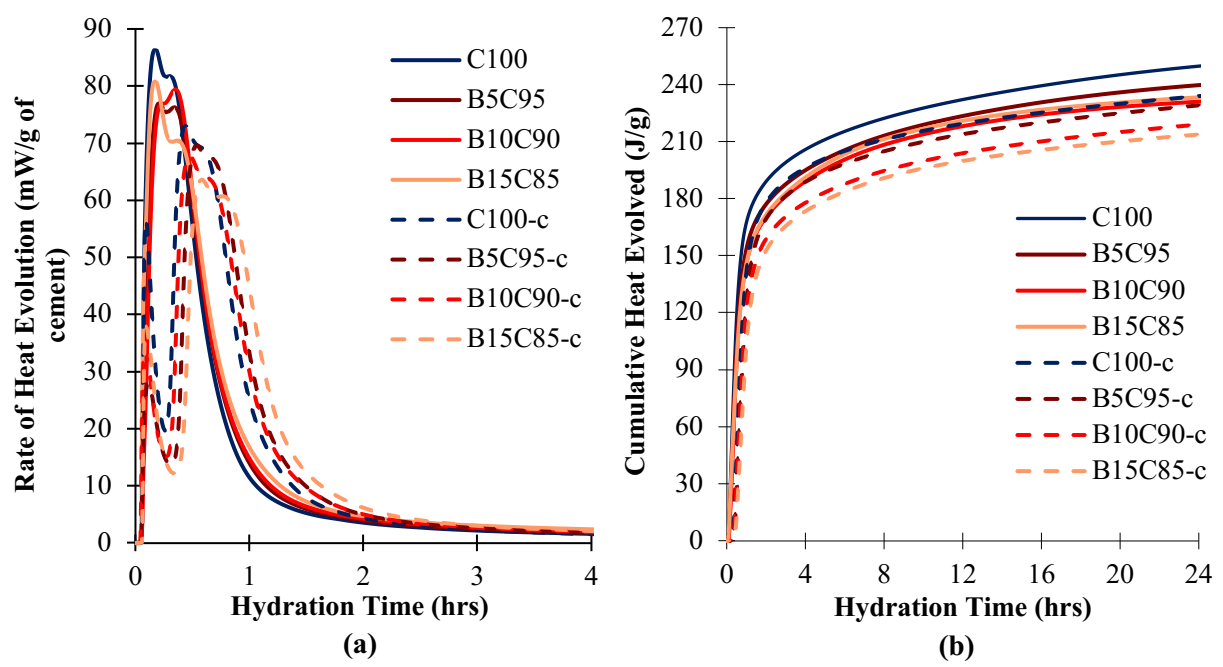


Figure 5: Hydration kinetics of CSA cement with biochar replacement level varying 0% to 15% and with and without citric acid: (a) Rate of heat evolution; (b) Cumulative heat evolution (A: raw algae, C: CSA cement, c: citric acid).

Table 4: Peak time of the heat evolution and cumulative heat at 24 h of CSA cement pastes with raw algae and biochar and with and without addition of citric acid.

	Time to peak heat		Cumulative heat
Sample	Minutes	% Compared to control	at 24 h (J/g)
C100	12	-	251
A5C95	12	0	252
A10C90	18	50	236
A15C85	24	100	216
B5C95	14.4	20	240
B10C90	17	42	231
B15C85	12.6	5	233
C100-c	30	-	234
A5C95-c	33.6	12	218
A10C90-c	48	60	200
A15C85-c	55.2	84	184
В5С95-с	33	10	229
В10С90-с	30	0	219
B15C85-c	36.6	22	214

Setting time results of the CSA cement samples with raw algae and biochar with and without citric acid are shown in **Figure 6a and b**. The results indicate that without citric acid, CSA cement completely hardens in 20 minutes (C100), while the addition of citric acid extended this to 40 minutes for the C100-c mixture. **Figure 6a** shows that mixtures with raw algae exhibited longer initial and final setting times than those with biochar, with a direct correlation between increased algae content and extended setting, aligning with the hydration kinetics observed in **Figures 4 and 5**. In contrast, varying biochar replacement levels did not lead to significant differences in setting times relative to the C100 sample. With citric acid present (**Figure 6b**), the control mixture (C100-c) displayed initial and final setting times that are very similar to those of biochar-containing mixtures, suggesting that biochar's effect on setting time may be minimal even when combined with citric acid. However, mixtures with raw algae, especially A15C85-c and A10C90-c, had notably extended setting times in comparison to the control, with the A15C85-c mixture demonstrating the longest delay. This indicates that citric acid tends to further prolong the setting times when used in combination with raw algae. Additionally, it is evident that the presence of citric acid exerted a greater effect on the final setting time than on the initial setting time within mixtures containing raw algae.

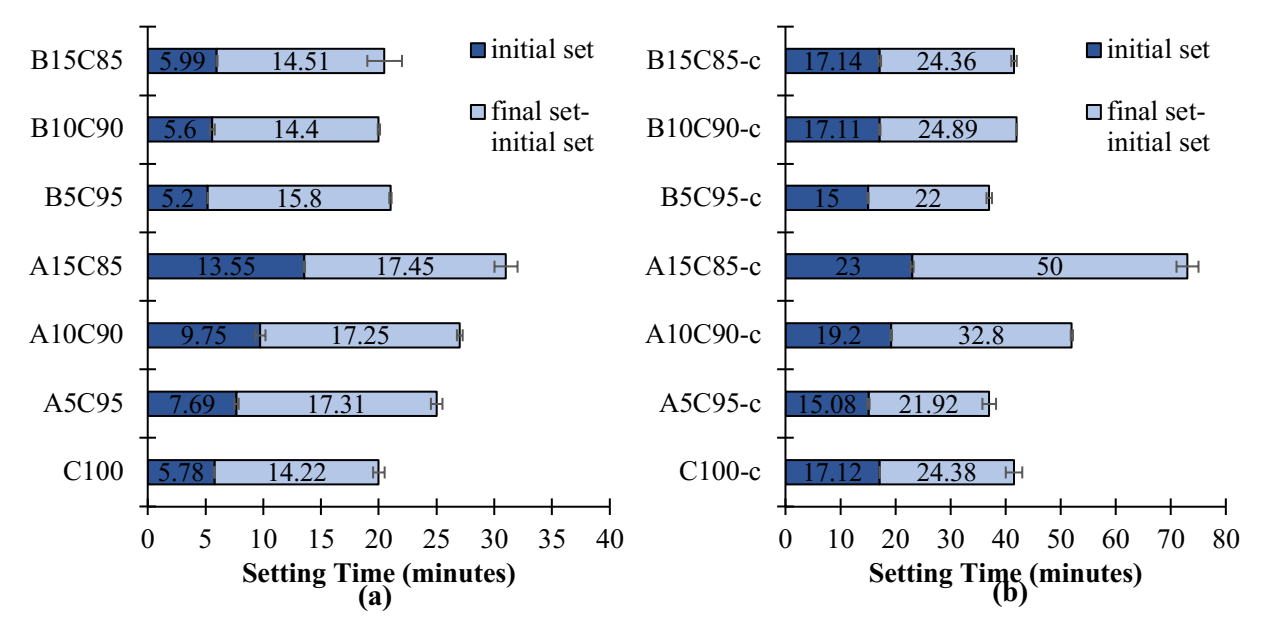


Figure 6: Setting time of CSA cement pastes with raw algae and biochar replacement levels varying from 0% to 15%: (a) without citric acid; (b) with citric acid (A: raw algae, B: biochar, C: CSA cement, c: citric acid).

To understand the effect of pH on the retardation of the 15% raw algae and 15% biochar additions, pH was tracked and compared with the heat evolution data. The pH of diluted CSA cement samples (at w/c=2.0) was tracked until the main hydration reaction was completed and samples started to harden.

Figure 7 shows the change in both pH and rate of heat evolution over time for C100, A15C85 and B15C85 samples. Initial pH was similar for all three samples, suggesting that addition of algae or biochar does not result in pH reductions in the hydrating CSA system. During the initial induction period pH decreased in all samples with the rate at the reductions in pH occurred linked to the retardation amount, with longer delays observed in the more retarded (C85A15) sample. With the acceleration of the rate of heat release reactions, pH simultaneously decreased, reaching a local minimum at the time of the peak heat release in all samples at 10 minutes for C100 and C85A15 samples and at 25 minutes for C85B15 samples. Decrease in pH correlated with the acceleration of hydration reactions, likely due to the consumption of hydroxyls by the ettringite [48]. After the start of the deceleration period pH began to

increase. With the increase of pH to approximately 10.3 and 11 in the samples, ettringite became more thermodynamically stable, and began to precipitate [49].

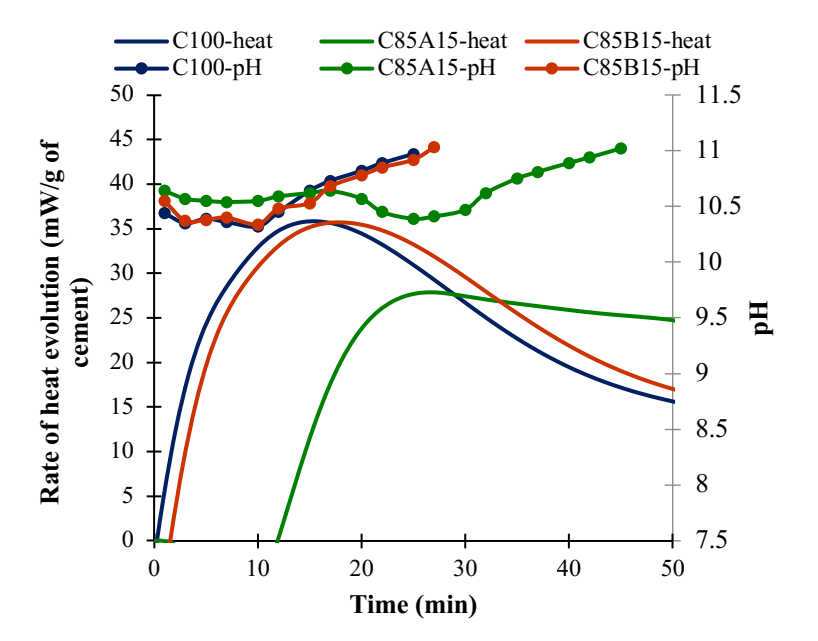


Figure 7: Rate of heat evolution vs pH in the diluted CSA cement pastes without and with 15% raw algae and biochar replacements.

## 3.2. Compressive Strength Development

Compressive strength development of 0.40 w/c CSA cement pastes with raw algae and biochar with and without citric acid is shown in **Figure 8a and b**. CSA cement with and without citric acid had significantly higher and earlier strength development than the OPC paste, shown with gray bars on both graphs. Incorporation of raw algae and biochar into CSA mixes, with and without citric acid, resulted in lower strength than the CSA cement control, as anticipated, suggesting that increasing replacement level leads to a decrease in the compressive strength. However, almost all raw algae and biochar samples (except C90A10-c and C85A15-c) generated significantly greater strength at 1-day compared to OPC sample due to the rapid strength gain and fast reactivity of CSA cement. Despite this early strength gain, the raw algae and biochar containing CSA cements displayed lower strength at 28 days than OPC.

The inclusion of raw algae and biochar samples without citric acid yielded similar strength development to each other across all testing days, and even slightly surpassed the strength of mixtures with citric acid. However, the majority of citric acid samples displayed delayed strength gain and did not attain comparable strength level as the no citric acid samples until 28 days, showing the slower reactivity and retardation effects of the citric acid. The C85A15-c sample exhibited the highest strength development among all other samples from 1 to 28 days, with a remarkable 158% increase in strength.

Comparing raw algae samples with citric acid to biochar samples with citric acid, the raw algae samples displayed slightly lower strength. This variance could be attributed to reduced workability, considering that the addition of raw algae samples had a more pronounced adverse impact on workability compared to biochar samples, leading to insufficient compaction. In the realm of biochar mixtures, the sample with 15% replacement level (C85B15-c) exhibited similar strength behavior to 5% addition, but significantly higher strength than 10% addition. Although some studies have highlighted the strength-improving

attributes of algal biomass by acting akin to internal curing agents or fillers [13, 17], no distinct strength enhancement trend was evident in these samples with increasing algae or biochar dosages. Despite the decrease in strength resulting from the addition of algae and biochar, it's important to emphasize that all the algae and biochar samples maintained commendable strengths within the range of 15 - 30 MPa. Additionally, these additives extended the casting and placing time significantly when compared to CSA cement without any additives.

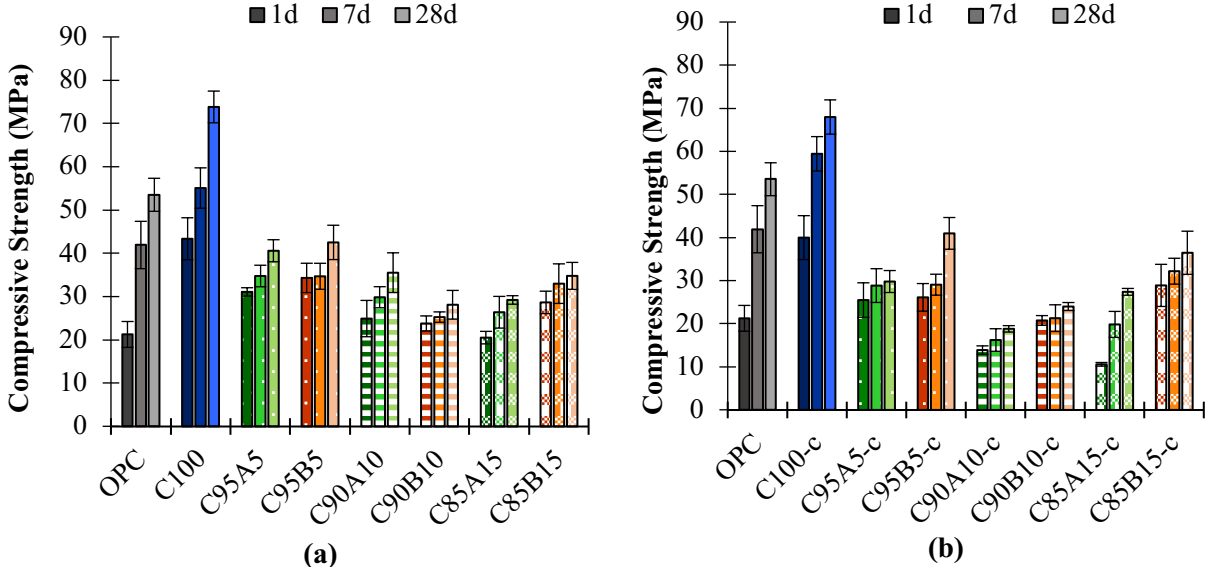


Figure 8: Compressive strength development of CSA cement pastes with raw algae and biochar replacement levels varying from 0% to 15%: (a) without citric acid; (b) with citric acid (A: raw algae, B: biochar, C: CSA cement, c: citric acid).

## 3.3. Microstructure Development

The mass loss percentage and differential mass loss curves of the control, 15% raw algae and 15% biochar samples with citric acid, at 1 and 28 days of hydration, obtained by TGA, are shown in Figure 9. The mass loss observed in the range of 25-150 °C is attributed to the dehydration of AFt & AFm whereas the mass loss between 150-250 °C is indicative of the presence of AH<sub>3</sub> present in the sample [8, 50]. On the differential thermogravimetric mass loss curve, the peak centered around 110 °C corresponds to the dehydration of calcium aluminate hydrate phases (AFt and AFm) and the peak around 220 °C corresponds to AH<sub>3</sub> [8, 51]. By analyzing the water loss associated with the dehydration of ettringite (32 moles of water), monosulfate (12 moles of water), and aluminum hydroxide (AH<sub>3</sub>) using TGA, the corresponding mass of the full molecule were calculated and the percent composition of each phase present in the sample were determined. Ettringite and monosulfate, challenging to differentiate in TGA due to overlapping dehydration temperature ranges, were assumed to exist in similar amounts as identified in a previous study by Winnefeld and Lothenbach [8]. According to that study, monosulfate forms after 1 or 4 days of hydration depending on the phase contents of CSA cement, representing 10% or 20% of the total calcium aluminate hydrate phases. Therefore, based on the composition of the CSA used in this study, it was assumed that monosulfate was formed after 4 days of hydration, making up 10% of the calcium aluminate hydrate phases.

Samples at 28 days of hydration displayed larger mass loss in the AFt & AFm region of the curve comparing their corresponding samples at 1 day of hydration, indicating that long-term curing resulted in increased hydrated AFt & AFm quantities relative to shorter curing periods. AH<sub>3</sub> quantities in all samples

were similar at both 1 and 28 days of hydration, suggesting that AH<sub>3</sub> phases primarily form during the first 24 hours of curing even with the addition of retardants.

**Figure 10** shows the formation of hydration products in the CSA samples throughout 28 days of curing. In all samples, both AFt & AFm and AH<sub>3</sub> amounts increased rapidly, leading to the formation of 95-100% of the final quantity of hydration products by 28 days within 1 day. The addition of 15% raw algae and biochar decreased the rate of AFt & AFm formation and resulted in lower ettringite formation compared to the control sample at both testing days. Moreover, biochar sample resulted in a slightly higher AFt & AFm production than the raw algae sample, which is correlated with the strength results **(Figure 8b)**. On the other hand, all samples contained very similar amounts of aluminum hydroxide from 1 to 28 days of hydration.

Despite the relatively lower quantities of AFt & AFm found in both raw algae and biochar samples, it is noteworthy that the biochar sample exhibited only a 12% reduction in AFt & AFm compared to the control sample, while the algae sample displayed a 16% decrease. This observation shows that although the addition of algal biomass tends to dilute the system and decreases the formation of hydration products, it does not seem to be as effective in inhibiting ettringite (AFt) formation as it is for C-S-H (calcium silicate hydrate) formation [13, 17, 30]. Thus, we confirmed the prior understanding that ettringite formation, from the reaction of tricalcium aluminate with gypsum and water, is not obstructed by the presence of carbohydrates found in *Chlorella* algae. On the other hand, the ettringite amount in the control sample exhibited a higher increase from day 1 to day 28 compared to the raw algae sample (10% increase in the control sample vs. 4% increase in the raw algae sample). This difference could be due to the prevention of further ettringite reactions and the transformation of ettringite into monosulfate within the system. Notably, negatively charged carbohydrates were observed to adsorb onto positively charged ettringite particles, effectively impeding their subsequent reactions [52]. Consequently, this mechanism may hinder complete hydration reactions, leading to reduced strength in samples containing algae.

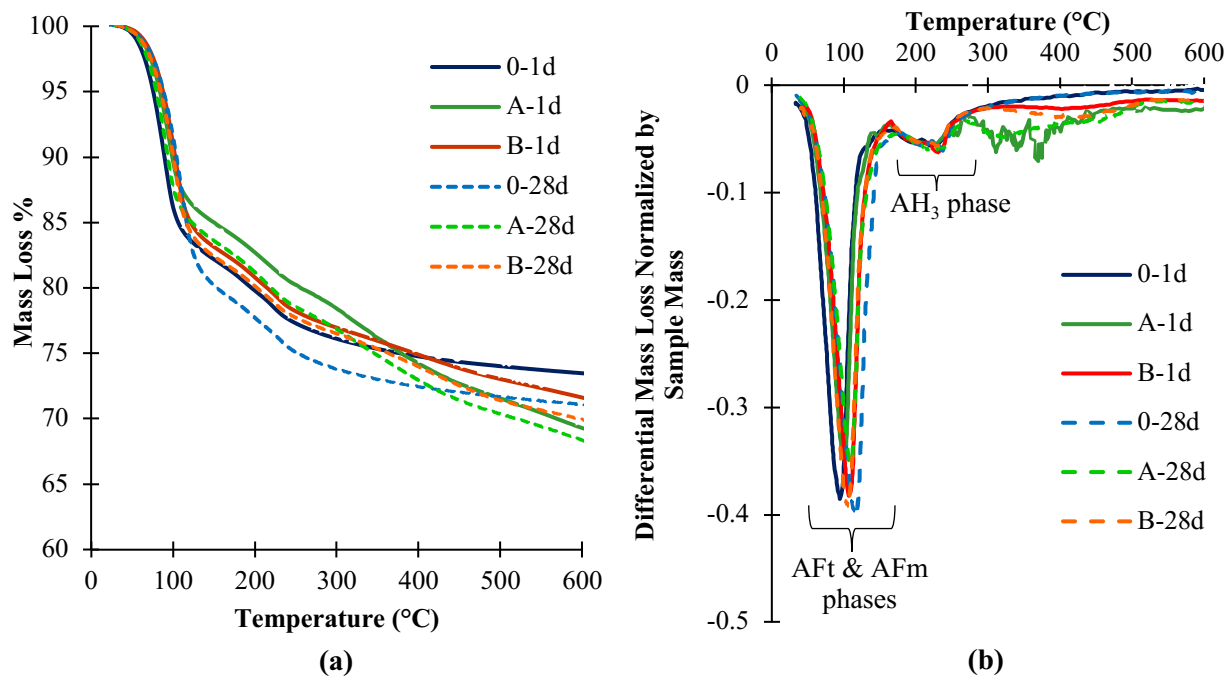


Figure 9: (a) Mass loss percentage curves, and (b) Differential thermogravimetric mass loss curves for CSA cement pastes of control, raw algae and biochar at 15% replacement level with citric acid (A: raw algae, B: biochar).

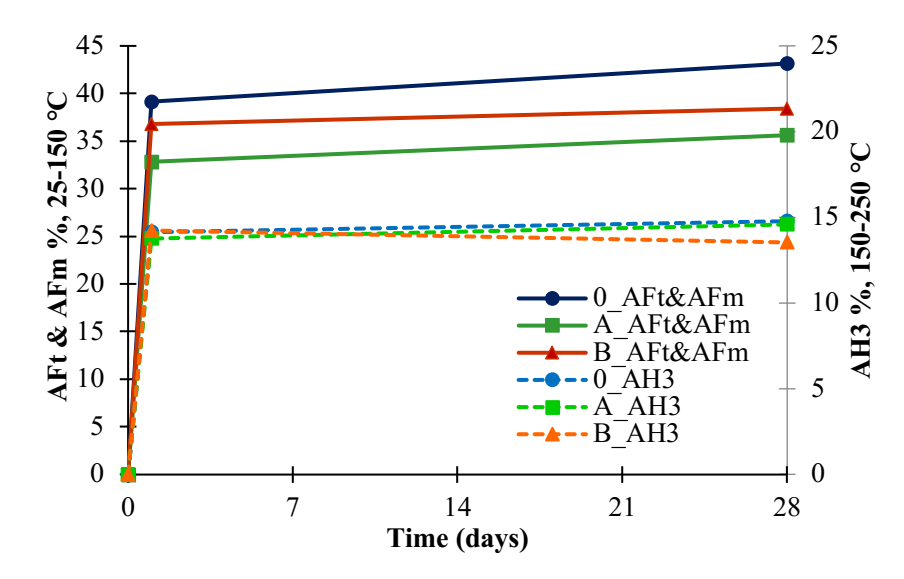


Figure 10: Evolution of AFt&AFm and AH<sub>3</sub> phases present in CSA samples of control, raw algae and biochar at 15% replacement level with citric acid, tracked by TGA (A: raw algae, B: biochar).

SEM images, in **Figure 11**, shows the morphology of CSA pastes without and with raw algae and biochar additions at 1 and 28 days of hydration. Raw algae and biochar were replaced by 15% of CSA cement. Overall, the addition of the raw algae and biochar does not appear to significantly change the microstructure development of the CSA cement paste and all samples had overall dense microstructures. However, cluster formation was observed in early age raw algae sample (A-1d), possibly due to the initial chemical interactions between the algae surface and the cement. Additionally, more needle-shaped ettringite formation was observed in the control and biochar samples compared to raw algae samples. Hydration from 1 to 28 days did not lead to significant alteration on the morphology of the samples, probably due to the rapid formation of the ettringite in CSA cement. At 28-days all samples exhibited similar morphologies with ettringite formation.

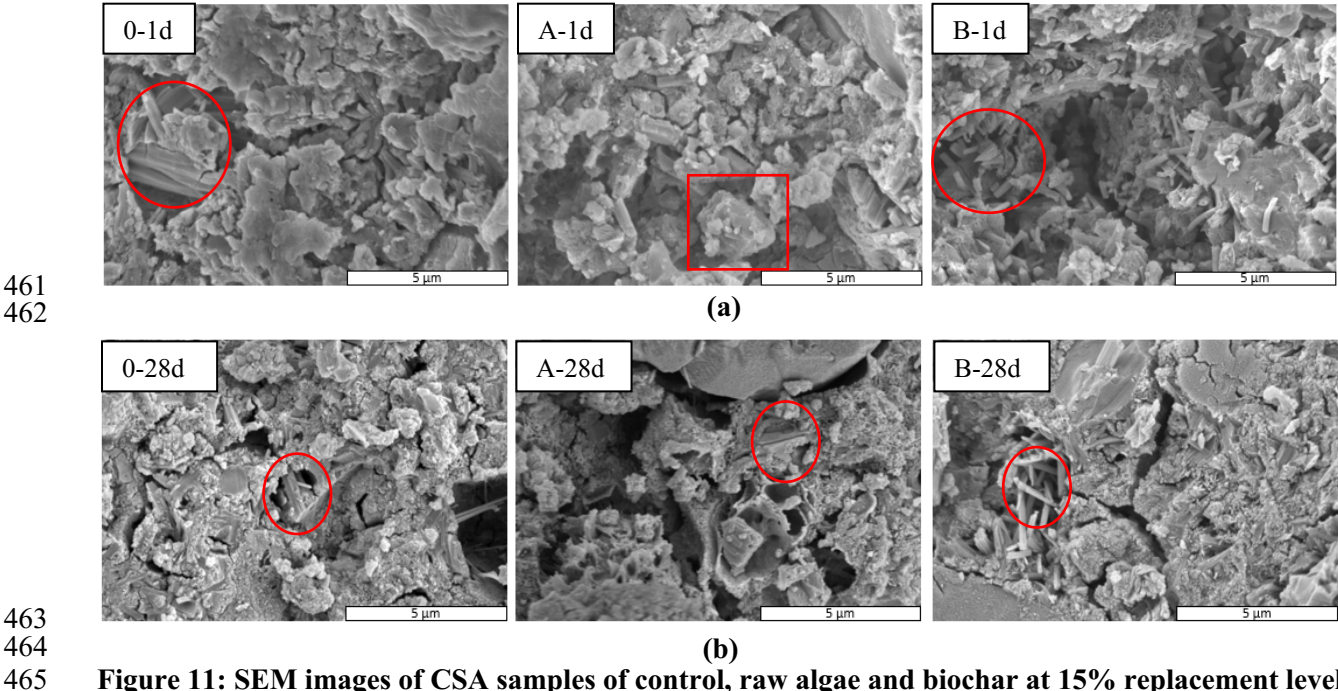


Figure 11: SEM images of CSA samples of control, raw algae and biochar at 15% replacement level with citric acid at (a) 1 day and (b) 28 days (0: control, A: raw algae, B: biochar). Circles show ettringite particles and squares show cluster formation.

## 3.4. Life Cycle Assessment

To assess the potential mitigation of cradle-to-gate embodied carbon emissions with biogenic carbon storage using algal biomass in CSA cement, the cradle-to-gate embodied carbon emissions and biogenic carbon storage were computed by performing a screening LCA of mix designs with different concentrations of raw algae and biochar in CSA cement. The results are shown in **Figure 12** for algae and biochar mixtures, using both mass-normalized and mass-compressive strength normalized units.

The results indicate that mixtures that include CSA cement had notably lower mass-normalized net CO<sub>2</sub> emissions when compared to OPC mixtures. The mass-normalized findings (**Figure 12a and c**) indicate that CSA cement with and without citric acid exhibited 30.3% and 28.7% lower mass-normalized net CO<sub>2</sub> emissions when compared to the OPC sample, respectively. However, when results incorporate functional performance and are normalized by both mass and compressive strength (**Figure 12b and d**), the reduction in net CO<sub>2</sub> emissions of CSA mixtures with and without citric acid compared to the OPC mixture were even higher at 49.5% and 43.9% lower than the OPC mixture, respectively.

The incorporation of algae-based admixtures within CSA cement yielded mixed results. In CSA cement mixtures without citric acid, replacing CSA cement with raw algae resulted in reduced mass-normalized net CO<sub>2</sub> emissions. Specifically, replacements of 5%, 10%, and 15% of algae corresponded to reductions of 17.5%, 35%, and 52.5%, respectively, when compared to the CSA control mixture. However, when these replacements are normalized by their 28-day compressive strength, they led to increases in net CO<sub>2</sub> emissions by 50%, 35.1%, and 20%, respectively, compared to the same CSA control mixture. Results with citric acid showed similar trends. This means that, although the CSA mixtures where algae replaced CSA cement had lower mass-normalized net CO<sub>2</sub> emissions relative to mixtures with 0% replacement, their reduction in functional performance (compressive strength) per unit mass outweighs their reduction

in emissions per unit mass. Thus, these initial results indicate that these mixtures may not necessarily be environmentally preferable when functional performance is considered.

The mixtures that include biochar replacement of CSA cement without citric acid, however, yielded different results due to greater biogenic carbon storage associated with biochar (see **Table 3**). Mixtures with biochar replacement of CSA cement in amounts of 5, 10, and 15% showed reductions in mass-normalized embodied carbon emissions of 24.7, 49.4, and 74.1%, respectively, when compared with the baseline CSA cement mixture without citric acid. However, changes in strength-normalized net CO<sub>2</sub> emissions were mixed, with a 30.7% increase, a 32.8% increase, and a 45.1% decrease, respectively. Similar to the algae results, the mixtures with biochar addition had lower mass-normalized net CO<sub>2</sub> emissions when compared to the pure CSA mixture, but the results for compressive strength normalized emissions were mixed. The 5% and 10% biochar replacement scenarios showed an increase in strength normalized emissions, but the 15% replacement scenario indicated a 45.1% reduction compared to the control CSA mixture without citric acid. A similar trend was indicated for the scenarios with citric acid. This demonstrates that the 15% biochar replacement scenarios may offer a lower global warming potential when compared with the comparable CSA scenarios that do not include any replacement with biochar, even when accounting for functional performance.

These findings highlight that, while the addition of raw algae and biochar can reduce mass-normalized cradle-to-gate embodied carbon emissions, that there may also be a loss in functional performance (compressive strength) when they are directly substituted for CSA cement. Certain mixtures, such as the CSA cement mixtures with 15% biochar replacement, warrant further consideration, as the results herein indicate that they may be environmentally preferable to the pure CSA cement mixtures due to their lower mass and mass-strength normalized embodied carbon emissions.

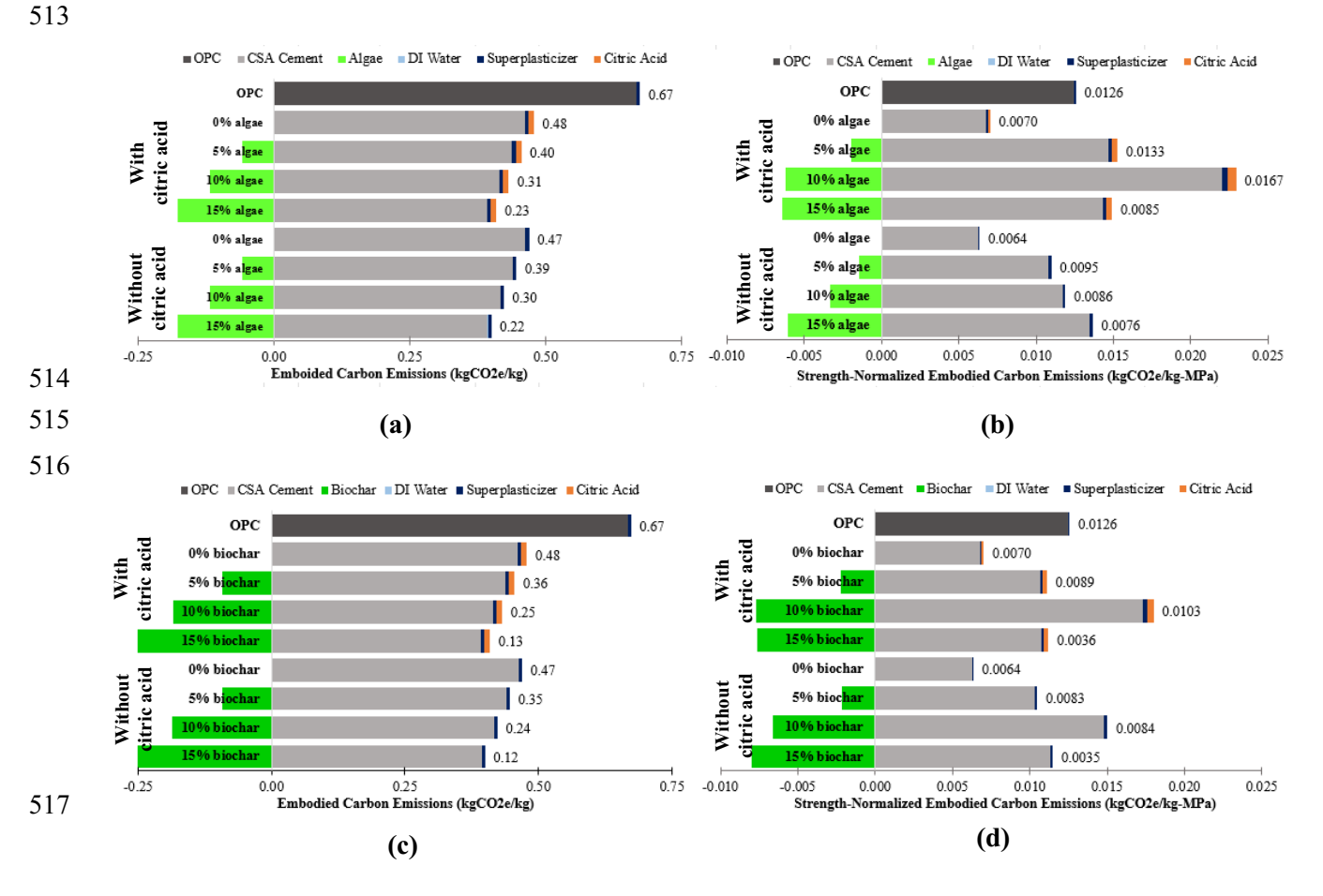


Figure 12: Embodied carbon emissions of OPC sample, CSA samples with raw algae (a,b) and biochar (c,d) at varying replacement levels with and without citric acid. Results are normalized based on both mass (kgCO<sub>2</sub>e/kg) (a, c) and both mass and 28-day compressive strength (kgCO<sub>2</sub>e/kg-MPa) (b, d). Negative values indicate biogenic carbon storage, while positive values indicate cradle-to-gate embodied carbon emissions. The net CO<sub>2</sub> emissions are shown to the right of each bar.

#### 4. Future Outlooks

518519

520

521

522

523

524525

526

527

528529

530

531

532

533

534

535

536

537

538

539

540

541

542

543

544

545

546

It was demonstrated that *Chlorella*, a typical class of algae, can induce a retarding effect on CSA cement hydration, both with and without citric acid. When replacing 10% and 15% of the cement with raw algal biomass, the peak of heat evolution was delayed by 50% and 100%, respectively, in comparison to samples without algae. The addition of citric acid further extended the timing of main heat release peak and setting time, effectively augmenting the retardation effect induced by raw algae. Considering its availability and sustainability due to CO<sub>2</sub>-storing potential, *Chlorella* algae has the potential to serve as a retarder for CSA cement. Although the biochar incorporation led to a lower amount of retardation compared to raw algae samples, it did not compromise strength to the same extent as raw algae. Notably, with the use of a minimal amount of citric acid (0.5% by cement weight), 15% biochar sample exhibited 67% longer hydration time in contrast to the control sample without citric acid.

In terms of environmental sustainability, the biogenic carbon storage of raw algae and biochar equates to approximately -1.8 kgCO<sub>2</sub>e/kg and -2.9 kgCO<sub>2</sub>e/kg, respectively. Considering that the embodied carbon emissions of OPC are 0.97 kgCO<sub>2</sub>e/kg and of CSA are 0.67 kgCO<sub>2</sub>e/kg, 15 % of algae and biochar replacements in CSA cement pastes would translate to reduction of 66% and 82% in embodied carbon emissions, respectively, when measured against OPC. However, direct substitution of CSA cement with raw algae can lead to a loss in functional performance (compressive strength), while 15% biochar replacement resulted in a better strength performance and a lower CO<sub>2</sub> emission. These results suggest that biochar could be effectively used in CSA cement as a sustainable approach in engineering practice. This conclusion aligns well with other efficiency enhancements seen in cement production, such as the energy efficiency benefits facilitated by the use of CSA cement when compared to OPC.

#### 5. Conclusion

- 547 This study investigated the effects of algal biomass, raw *Chlorella* algae and its heat-treated form
- 548 (biochar), on fresh and hardened properties of CSA cement, a sustainable alternative to OPC. CSA
- cement was replaced with algal biomass at varying percentages 0, 5, 10, and 15% to explore effects of
- algal biomass replacement on hydration kinetics, microstructure development, and compressive strength.
- Experimental results showed that increasing raw algae dosage led to a proportional retardation in the
- hydration. Specifically, the addition of 10 and 15% raw algal biomass delayed hydration by 50% and
- 553 100%, respectively, compared to samples without algae. However, the retardation amount was limited in
- these samples, as raw algae is found to mainly retard hydration of alite phase, which is not present in CSA
- cement. On the other hand, addition of biochar in same percentages, the retardation effect was not
- observed. This shows that the retardation in raw algae is due to the presence of hydroxyl and carboxyl
- functional groups that decompose upon heating to obtain biochar.
- Delays in cement hydration due to the incorporation of raw algal biomass resulted in lower compressive
- strengths, as anticipated. However, the strengths were comparable with the OPC mixtures, owing to the
- inherently high compressive strengths of CSA cement. Samples with raw algae and citric acid showed
- slightly lower strengths compared to those with biochar and citric acid. When considering the
- 562 microstructure development, TGA analyses demonstrated rapid increases in the quantities of hydration
- products (ettringite/monosulfate and aluminum hydroxide) in 15% raw algae and 15% biochar samples,
- leading to the formation of 95-100% of the 28-day quantity of these products within 1 day. However, the

- rate of ettringite/monosulfate formation decreased in these samples compared to the control sample at
- both testing days, probably due to the limited ettringite to monosulfate transformation.
- Lastly, LCA was employed to estimate the cradle-to-gate embodied carbon emissions and biogenic
- carbon storage for each mix design using both mass-normalized and mass-strength normalized units. The
- results showed that all raw algae samples had 17% to 51% lower net CO<sub>2</sub> emissions, depending on the
- 570 replacement amount, in comparison to non-biogenic samples. Similarly, all biochar samples exhibited a
- reduction of 25% to 73% in CO<sub>2</sub>e emissions. However, biochar samples performed better compared to
- raw algae samples when normalized strength performance was considered.

## 573 **6. Acknowledgements**

- 574 This research was made possible by the Department of Civil, Environmental, and Architectural
- 575 Engineering, the College of Engineering and Applied Sciences, and the Living Materials Laboratory
- 576 (LMLab) at the University of Colorado Boulder with financial support from the National Science
- 577 Foundation (Award No. CMMI-1943554). This research was supported in part by the Colorado Shared
- 578 Instrumentation in Nanofabrication and Characterization (COSINC-CHR) within the College of
- 579 Engineering and Applied Science, University of Colorado Boulder. The authors would like to
- acknowledge the support of the staff (Tomoko Borsa) and the facility that made this work possible. The
- authors would also like to acknowledge Matthew Fyfe, Caitlin Adams, and Samuel Armistead for
- reviewing and proofreading the manuscript.

#### 583 7. References

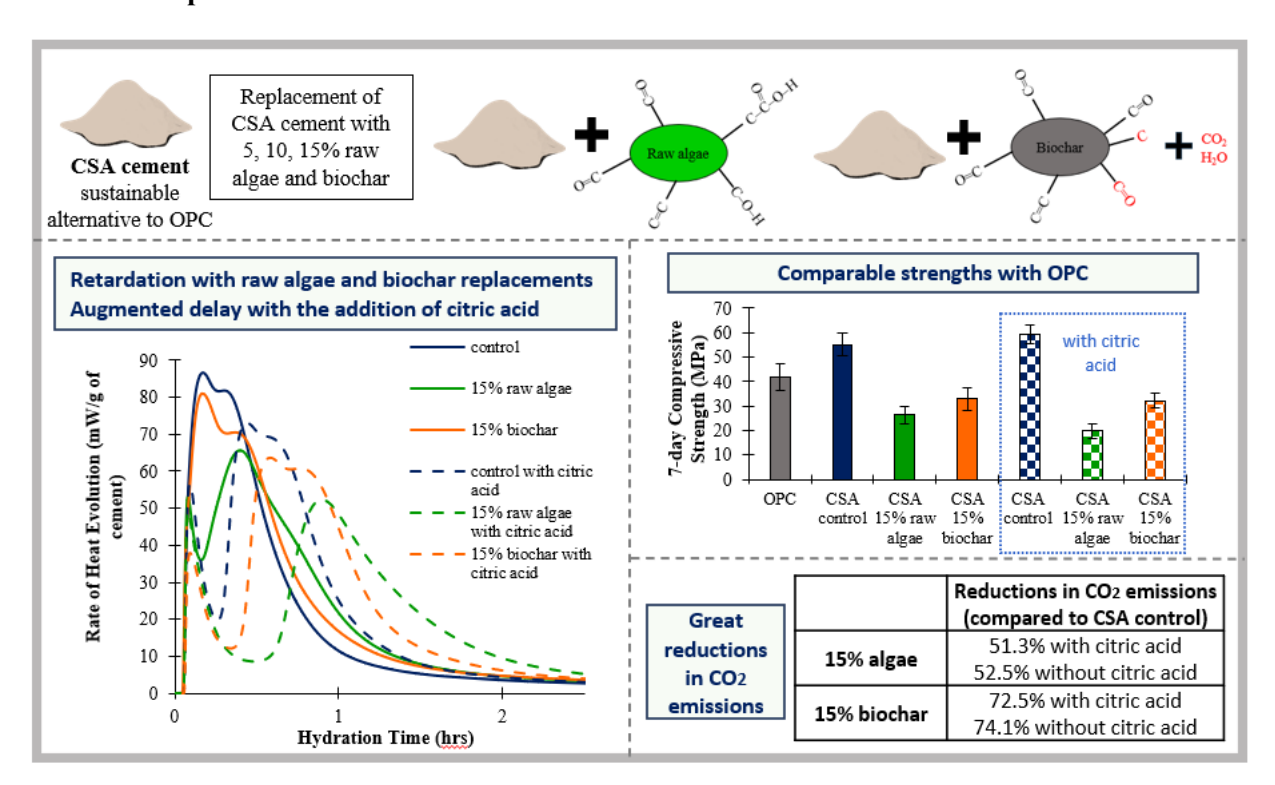
- [1] C. Shi, A. F. Jim'enez, and A. Palomo, "New cements for the 21st century: The pursuit of an
- alternative to portland cement," Cement and concrete research, vol. 41, no. 7, pp. 750–763, 2011.
- 586 [2] M. Juenger, F. Winnefeld, J. L. Provis, and J. Ideker, "Advances in alternative cementitious binders,"
- 587 Cement and concrete research, vol. 41, no. 12, pp. 1232–1243, 2011.
- 588 [3] F. P. Glasser and L. Zhang, "High-performance cement matrices based on calcium sulfoaluminate—
- belite compositions," Cement and Concrete Research, vol. 31, no. 12, pp. 1881–1886, 2001.
- 590 [4] J. Pera and J. Ambroise, "New applications of calcium sulfoaluminate cement," Cement and concrete
- 591 research, vol. 34, no. 4, pp. 671–676, 2004.
- 592 [5] Q. Zhou, N. Milestone, and M. Hayes, "An alternative to portland cement for waste encapsulation—
- the calcium sulfoaluminate cement system," Journal of hazardous materials, vol. 136, no. 1, pp. 120–129,
- 594 2006.
- 595 [6] L. Pelletier, F. Winnefeld, and B. Lothenbach, "The ternary system portland cement-calcium
- sulphoaluminate clinker–anhydrite: hydration mechanism and mortar properties," Cement and Concrete
- 597 Composites, vol. 32, no. 7, pp. 497–507, 2010.
- 598 [7] L. E. Burris and K. E. Kurtis, "Influence of set retarding admixtures on calcium sulfoaluminate
- cement hydration and property development," Cement and Concrete Research, vol. 104, pp. 105–113,
- 600 2018.
- 601 [8] F. Winnefeld and B. Lothenbach, "Hydration of calcium sulfoaluminate cements experimental
- findings and thermodynamic modelling," Cement and Concrete Research, vol. 40, no. 8, pp. 1239–1247,
- 603 2010
- [9] I. A. Chen, C. W. Hargis, and M. C. Juenger, "Understanding expansion in calcium sulfoaluminate—
- belite cements," Cement and Concrete Research, vol. 42, no. 1, pp. 51–60, 2012.

- [10] Y. Liao, X. Wei, and G. Li, "Early hydration of calcium sulfoaluminate cement through electrical
- 607 resistivity measurement and microstructure investigations," Construction and Building Materials, vol. 25,
- 608 no. 4, pp. 1572–1579, 2011.
- 609 [11] C. W. Hargis, A. Telesca, and P. J. Monteiro, "Calcium sulfoaluminate (ye'elimite) hydration in the
- presence of gypsum, calcite, and vaterite," Cement and Concrete Research, vol. 65, pp. 15–20, 2014.
- 611 [12] A. Telesca, M. Marroccoli, M. Pace, M. Tomasulo, G. Valenti, and P. Monteiro, "A hydration study
- of various calcium sulfoaluminate cements," Cement and Concrete Composites, vol. 53, pp. 224–232,
- 613 2014.
- 614 [13] X. Chen, M. G. Matar, D. N. Beatty, and W. V. Srubar III, "Retardation of portland cement
- 615 hydration with photosynthetic algal biomass," ACS Sustainable Chemistry & Engineering, vol. 9, no. 41,
- 616 pp. 13726–13734, 2021.
- 617 [14] S. Gupta and H. W. Kua, "Carbonaceous micro-filler for cement: Effect of particle size and dosage
- of biochar on fresh and hardened properties of cement mortar," Science of the Total Environment, vol.
- 619 662, pp. 952–962, 2019.
- 620 [15] S. Gupta, H. W. Kua, and H. J. Koh, "Application of biochar from food and wood waste as green
- admixture for cement mortar," Science of the total environment, vol. 619, pp. 419–435, 2018.
- [16] S. Gupta, H. W. Kua, and C. Y. Low, "Use of biochar as carbon sequestering additive in cement
- mortar," Cement and concrete composites, vol. 87, pp. 110–129, 2018.
- 624 [17] M.-Y. Lin, P. Grandgeorge, A. M. Jimenez, B. H. Nguyen, and E. Roumeli, "Long-term hindrance
- effects of algal biomatter on the hydration reactions of ordinary portland cement," ACS Sustainable
- 626 Chemistry & Engineering, vol. 11, pp. 8242-8854, 2023.
- 627 [18] D. Cuthbertson, U. Berardi, C. Briens, and F. Berruti, "Biochar from residual biomass as a concrete
- filler for improved thermal and acoustic properties," Biomass and bioenergy, vol. 120, pp. 77–83, 2019.
- 629 [19] I. Michalak and K. Chojnacka, "Introduction: Toward algae-based products," Algae biomass:
- characteristics and applications: towards algae-based products, pp. 1–5, 2018.
- 631 [20] T. Yuan, A. Tahmasebi, and J. Yu, "Comparative study on pyrolysis of lignocellulosic and algal
- biomass using a thermogravimetric and a fixed-bed reactor," Bioresource Technology, vol. 175, pp. 333–
- 633 341, 2015.
- 634 [21] Y. Chisti, "Biodiesel from microalgae," Biotechnology advances, vol. 25, no. 3, pp. 294–306, 2007.
- [22] J. Liu, C. Shi, X. Ma, K. H. Khayat, J. Zhang, and D. Wang, "An overview on the effect of internal
- curing on shrinkage of high performance cement-based materials," Construction and Building Materials,
- 637 vol. 146, pp. 702–712, 2017.
- 638 [23] E. Hernandez, P. d. J. Cano-Barrita, and A. Torres-Acosta, "Influence of cactus mucilage and marine
- brown algae extract on the compressive strength and durability of concrete," Materiales de Construcci´on,
- 640 vol. 66, no. 321, pp. e074–e074, 2016.
- [24] H. Maljaee, R. Madadi, H. Paiva, L. Tarelho, and V. M. Ferreira, "Incorporation of biochar in
- cementitious materials: A roadmap of biochar selection," Construction and Building Materials, vol. 283,
- 643 p. 122757, 2021.
- 644 [25] A.-M. Poppe and G. De Schutter, "Cement hydration in the presence of high filler contents," Cement
- and Concrete Research, vol. 35, no. 12, pp. 2290–2299, 2005.
- [26] X. Gong, B. Zhang, Y. Zhang, Y. Huang, and M. Xu, "Investigation on pyrolysis of low lipid
- microalgae chlorella vulgaris and dunaliella salina," Energy & fuels, vol. 28, no. 1, pp. 95–103, 2014.

- 648 [27] B. C. Acarturk and L. E. Burris, "Investigations of the optimal requirements for curing of calcium
- sulfoaluminate cement systems," CEMENT, vol. 12, p. 100072, 2023.
- 650 [28] A. Simonovicova, A. Takacova, I. Simkovic, and S. Nosalj, "Experimental treatment of hazardous
- ash waste by microbial consortium aspergillus niger and chlorella sp.: Decrease of the ni content and
- 652 identification of adsorption sites by fourier-transform infrared spectroscopy," Frontiers in Microbiology,
- 653 vol. 12, p. 792987, 2021.
- 654 [29] D. Marchon and R. Flatt, "Impact of chemical admixtures on cement hydration," in Science and
- technology of concrete admixtures, pp. 279–304, 2016.
- 656 [30] O. Chaudhari, J. J. Biernacki, and S. Northrup, "Effect of carboxylic and hydroxycarboxylic acids on
- cement hydration: experimental and molecular modeling study," Journal of Materials Science, vol. 52, pp.
- 658 13719–13735, 2017.
- 659 [31] ASTM C1679: "Standard practice for measuring the hydration kinetics of hydraulic cementitious
- mixtures using isothermal calorimetry," ASTM International, 2014.
- [32] ASTM C305: "Standard practice for mechanical mixing of hydraulic cement pastes and mortars,"
- ASTM International, 2016.
- [33] ASTM C191: "Standard test methods for time of setting of hydraulic cement by Vicat needle,"
- ASTM International, 2019.
- 665 [34] ASTM C109: Standard test method for compressive strength of hydraulic cement mortars (using 2-
- in. or [50-mm] cube specimens," ASTM International, 2016.
- [35] J. Zhang and G. W. Scherer, "Comparison of methods for arresting hydration of cement," Cement
- and Concrete Research, vol. 41, no. 10, pp. 1024–1036, 2011.
- [36] S. Luo, M. Liu, L. Yang, and J. Chang, "Effects of drying techniques on the crystal structure and
- morphology of ettringite," Construction and Building Materials, vol. 195, pp. 305–311, 2019.
- [37] M. Liu, S. Luo, L. Yang, and J. Ren, "Influence of water removal techniques on the composition and
- microstructure of hardened calcium sulfoaluminate cement pastes," Materials and Structures, vol. 53, pp.
- 673 1–11, 2020.
- [38] ISO 14040: 2006-environmental management-life cycle assessment-principles and framework,"
- 675 2006.
- 676 [39] "ISO 14044: 2006-environmental management-life cycle assessment-requirements and guidelines,"
- 677 2006
- 678 [40] A. Levasseur, P. Lesage, M. Margni, and R. Samson, "Biogenic carbon and temporary storage
- addressed with dynamic life cycle assessment," Journal of Industrial Ecology, vol. 17, no. 1, pp. 117–128,
- 680 2013.
- [41] G. Hammond and C. Jones, Inventory of carbon & energy version 3.0. 2019.
- 682 [42] One Click LCA Ltd., "One click LCA." https://www.oneclicklca.com. Last accessed on 18 August
- 683 2023.
- 684 [43] CTS Cement, "Environmental product decleration."
- https://www.ctscement.com/assets/doc/info/EPDlabel RapidSet Labeling Sustainability CTS Cement.p
- df. Last accessed on 18 August 2023.
- 687 [44] J. Wang, Z. Cui, Y. Li, L. Cao, and Z. Lu, "Techno-economic analysis and environmental impact
- assessment of citric acid production through different recovery methods," Journal of Cleaner Production,
- 689 vol. 249, p. 119315, 2020.

- 690 [45] S. L. Williams, Use of Siliceous and Calcareous Microalgae to Decarbonize Cement Production.
- 691 PhD thesis, University of Colorado at Boulder, 2022.
- 692 [46] H. Nguyen, W. Kunther, K. Gijbels, P. Samyn, V. Carvelli, M. Illikainen, and P. Kinnunen, "On the
- retardation mechanisms of citric acid in ettringite-based binders," Cement and Concrete Research, vol.
- 694 140, p. 106315, 2021.
- 695 [47] A. Cody, H. Lee, R. Cody, and P. Spry, "The effects of chemical environment on the nucleation,
- 696 growth, and stability of ettringite [ca3al (oh) 6] 2 (so4) 3· 26h2o," Cement and Concrete Research, vol.
- 697 34, no. 5, pp. 869–881, 2004.
- 698 [48] P. Akula and D. N. Little, "Mineralogical characterization and thermodynamic modeling of
- 699 synthesized ettringite from ca-al-so4 suspensions," Construction and Building Materials, vol. 269, p.
- 700 121304, 2021.
- 701 [49] A. Gabrisova, J. Havlica, and S. Sahu, "Stability of calcium sulphoaluminate hydrates in water
- solutions with various ph values," Cement and Concrete Research, vol. 21, no. 6, pp. 1023–1027, 1991.
- 703 [50] S. Tang, H. Zhu, Z. Li, E. Chen, and H. Shao, "Hydration stage identification and phase
- transformation of calcium sulfoaluminate cement at early age," Construction and Building Materials, vol.
- 76 75, pp. 11–18, 2015.
- [51] B. Lothenbach, P. Durdzinski, and K. De Weerdt, "Thermogravimetric analysis," A practical guide to microstructural analysis of cementitious materials, vol. 1, pp. 177-211, 2016.
- 709 [52] B. J. Smith, A. Rawal, G. P. Funkhouser, L. R. Roberts, V. Gupta, J. N. Israelachvili, and B. F.
- 710 Chmelka, "Origins of saccharide-dependent hydration at aluminate, silicate, and aluminosilicate
- surfaces," Proceedings of the National Academy of Sciences, vol. 108, no. 22, pp. 8949–8954, 2011.

## **Abstract Graphic**



712713

- 715 Synopsis
- 716 This study reports eco-friendly innovations in concrete, using algae-based additives in environmentally
- 717 friendly calcium sulfoaluminate cement to reduce carbon dioxide emissions and enhance sustainability.